

Very forward phenomena in pA and UPC

Mark Strikman, PSU

Focus on two motivations

Studying structure of proton, photon beyond single parton distributions GPD... — fluctuations

Small x - perturbative small x regime - competition of DGLAP and BFKL - resummation

very forward detector would allow to reach $x \sim 10^{-6} \div 10^{-7}$

- Black disk limit (limit of 100% absorption) / saturation effects due to the small x effects: in proton - proton/nucleus collisions a parton with given x_1 resolves partons in another nucleon/nucleus down to $x_2 = 4p_{\perp}^2/x_1s$

At LHC $x_1 = 0.1, p_{\perp} = 2\text{GeV}/c \longrightarrow x_{2min} = 10^{-6}$

Near GZK $x_1 = 0.1, p_{\perp} = 2\text{GeV}/c \longrightarrow x_{2min} = 10^{-9}$

If the logic of propagation of fast partons through strong fields is generically correct should see plenty of effects in pA collisions in the p fragmentation

implications for GZK protons

Adrian's talk

best to have as large x_1 as possible

For ultraperipheral collisions $x_{2min} \sim 10^{-4}, 10^{-5}$ depending on the probe

High energy scanning - step I - one D scan

PDFs

High energy scanning - step II - three D scan

GPDs

***High energy scanning - step III - parton -
parton correlations in transverse plane***

**Multiparton interactions (pp, pA) – mean field works for
 $x < 0.01$ - difficult to reconcile with dominance of hot spots at $Q_0 \sim 1$ GeV scale**

We focus on Global correlations: x - & transverse size

Space - time picture of high energy pA collisions

Fluctuations of overall strength of high energy NN interaction



High energy projectile stays in a frozen configuration distances $l_{\text{coh}} = c\Delta t$

$$\Delta t \sim 1/\Delta E \sim \frac{2p_h}{m_{\text{int}}^2 - m_h^2}$$

At LHC for $m_{\text{int}}^2 - m_h^2 \sim 1\text{GeV}^2$ $l_{\text{coh}} \sim 10^7 \text{ fm} \gg 2R_A \gg 2r_N$

coherence up to $m_{\text{int}}^2 \sim 10^6 \text{ GeV}^2$

Hence system of quarks and gluons passes through the nucleus interacting essentially with the same strength but changes from one event to another different strength



Strength of interaction of white small system is proportional to the area occupies by color.

QCD factorization theorem for the interaction of small size color singlet wave package of quarks and gluons.

For small quark - antiquark dipole $\sigma(q\bar{q}T) = \frac{\pi^2}{3} r_{tr}^2 x g_T(x, Q^2 = \lambda/r_t^2) \alpha_s(Q^2)$

small but rapidly growing with energy

For small 3 quark tripole

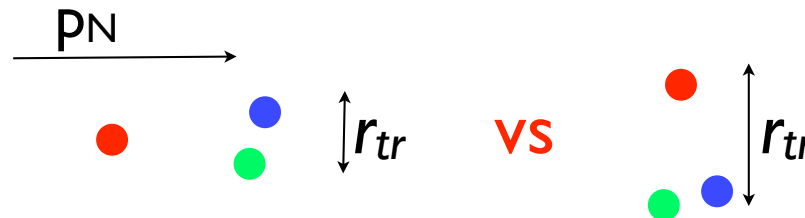
$$r_{tr}^2 \rightarrow (r_1 - (r_2 + r_3)/2)^2 + (r_2 - (r_1 + r_3)/2)^2 + (r_3 - (r_1 + r_2)/2)^2$$

dependence of $\sigma_{tot}(hN)$ on size holds also in the nonperturbative regime

$$\sigma_{tot}(KN) < \sigma_{tot}(\pi N)$$

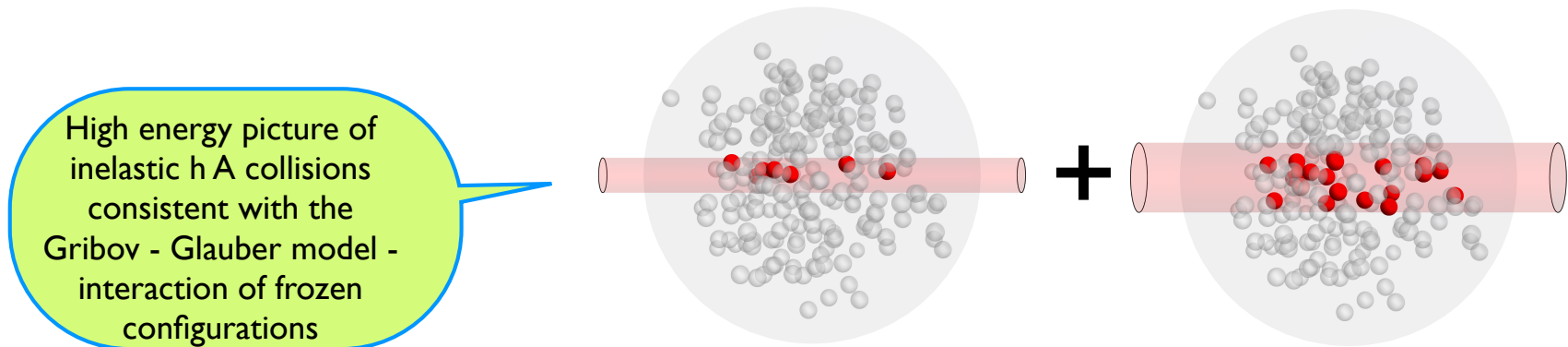
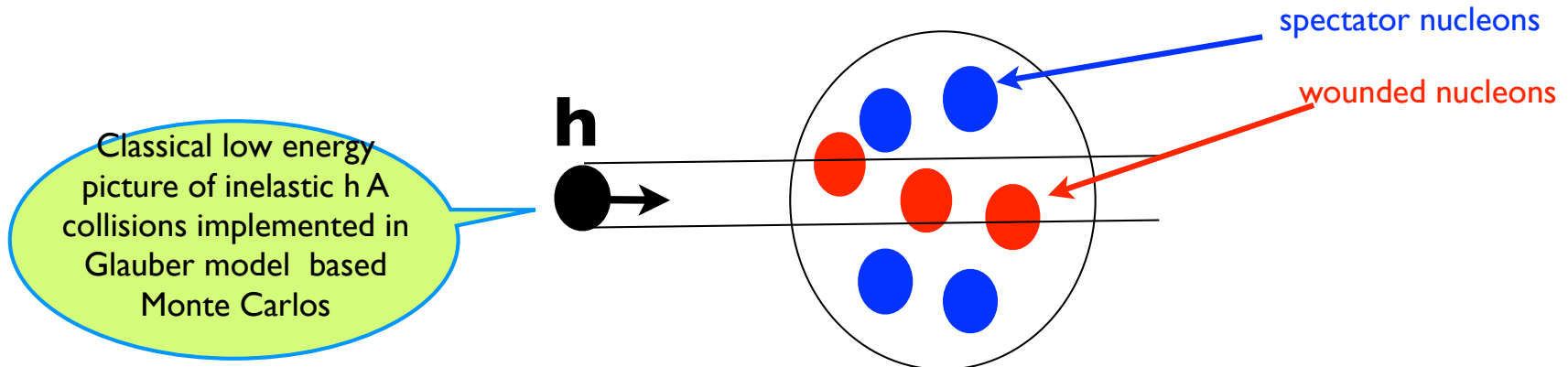
Global fluctuations of the strength of interaction of a fast nucleon/pion/photon, can originate from fluctuations of the overall size /shape, number of constituents.

Example: quark -diquark model of nucleon, junction?



We will refer fluctuations of the strength of interaction of nucleon, photon,.. as **color fluctuations of interaction strength** - studying them allows to go beyond single parton 3-D mapping of the nucleon

Constructive way to account for coherence of the high-energy dynamics is **Fluctuations of interaction = cross section fluctuation formalism**. Analogy: consider throwing a stick through a forest - with random orientation relative to the direction of motion. (No rotation while passing through the forest - large l_{coh} .) Different absorption for different orientations.

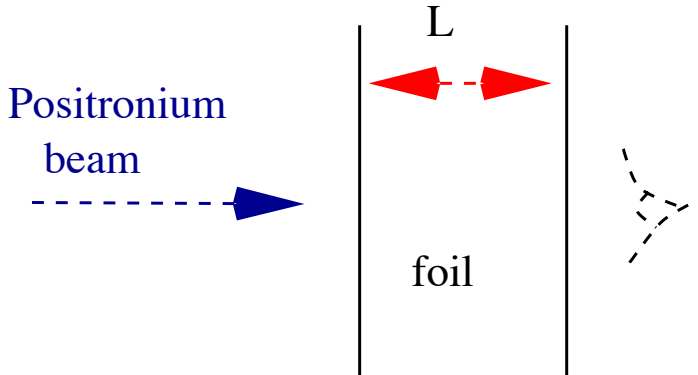


Expect effects similar positronium example = correlation between size and number of wounded nucleons

Instructive example: propagation of a very fast positronium (bound state of electron and positron) through a foil

first qualitative discussion - Nemenov, 1981, quantitative treatment Frankfurt and MS 91)

$$\frac{P_{pos}}{2m_e} \cdot \frac{1}{\Delta E(\sim \text{few } m_e \alpha^2)} \gg L(\text{foil})$$



For the positronium at high energies transverse size is frozen during traversing through the foil - so interaction is of dipole-dipole type $\sigma(d) \propto d^2$ where $d = r_t^e - r_t^{e+}$

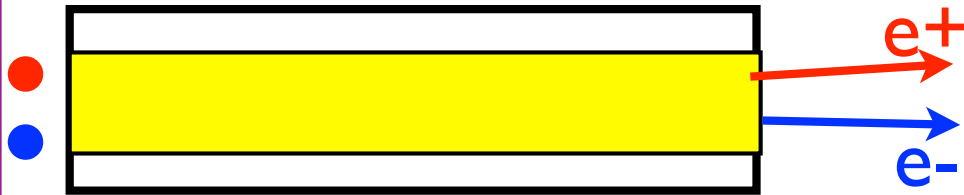
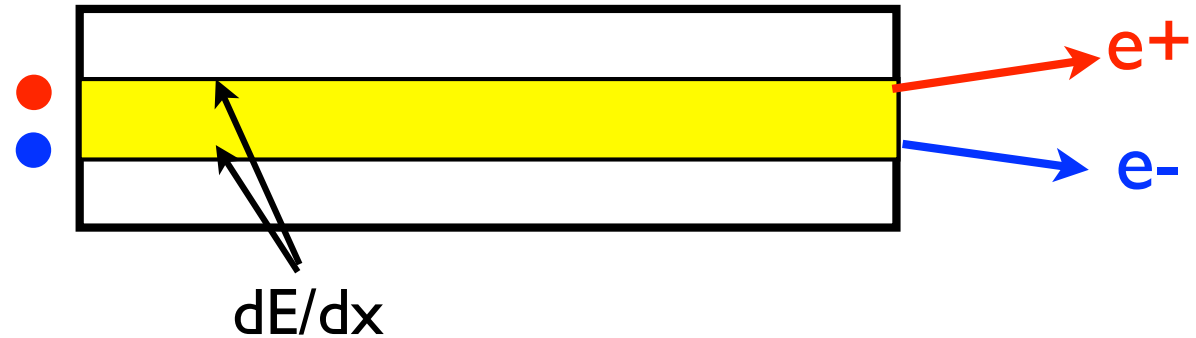
Amplitude of **i** → **f** transition: $|M_{if}| = \left[\int d^3r \Psi_{pos} \Psi_f^* \exp(-\sigma(d)\rho L/2) \right]^2$

For large **L**: survival probability $\frac{16}{(\langle \sigma \rangle \rho L)^2}$ absorption is not exponential !!!

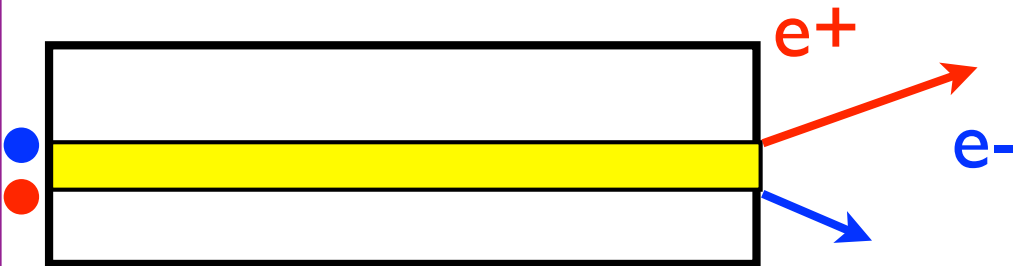
Even larger probability to transform to electron - positron pair $\frac{2}{\langle \sigma \rangle \rho L}$ of the same momentum as positronium

QED example, relevant for pA effects discussed later

Average configuration of incoming positronium



Post selection / Trigger on large d - large energy release along the path in the media - selects smaller than average transverse and longitudinal momenta in positronium - longitudinal momenta of electrons in the positronium fragmentation are softer ($x-1/2$ closer to 0) - looks as energy loss - but actually post selection.



Trigger on high p_t electron or electron with $x > 1/2$ (fraction of momentum of positronium carried by electron post selects events where excitations along the path were small.

Convenient quantity - $P(\sigma)$ -probability that hadron/photon interacts with cross section σ with the target.

$$\int P(\sigma) d\sigma = 1, \quad \int \sigma P(\sigma) d\sigma = \sigma_{tot},$$

$$\text{cf } P_{\text{MC Glauber}}(\sigma) = \delta(\sigma - \sigma_{tot})$$

$$\left. \frac{\frac{d\sigma(pp \rightarrow X+p)}{dt}}{\frac{d\sigma(pp \rightarrow p+p)}{dt}} \right|_{t=0} = \frac{\int (\sigma - \sigma_{tot})^2 P(\sigma) d\sigma}{\sigma_{tot}^2} \equiv \omega_{\sigma} \quad \begin{array}{l} \text{variance} \\ \text{Pumplin \& Miettinen} \end{array}$$

Good - Walker mode of coherent scattering Eigen states!

Warning - connection between fluctuations and inelastic diffraction is a reasonable model for $t=0$. However at finite t knockout mechanism becomes important and ultimately dominant

Example $\sigma(\text{Deuteron} + h \rightarrow (pn) + h) = 0$ for $t=0$ in the impulse approximation (no fluctuations) and not suppressed for $-t > 1/r_N^2$ - knockout mechanism

$$\int (\sigma - \sigma_{tot})^3 P(\sigma) d\sigma = 0,$$

$$P(\sigma)|_{\sigma \rightarrow 0} \propto \sigma^{n_q - 2}$$

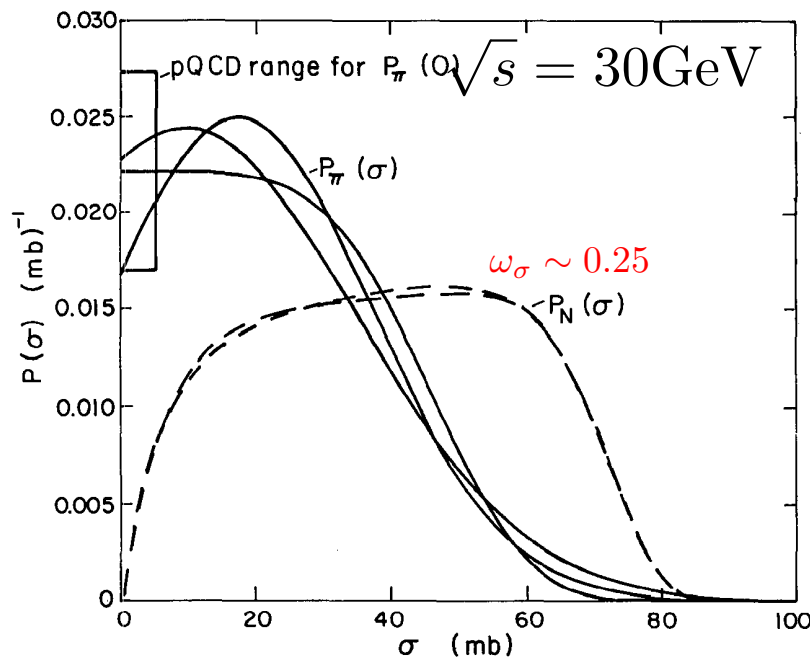
Baym et al from pD diffraction

Baym et al 1993 - analog of QCD counting rules
probability for all constituents to be in a small transverse
area

+ additional consideration that *for a many body system fluctuations near average value should be Gaussian*

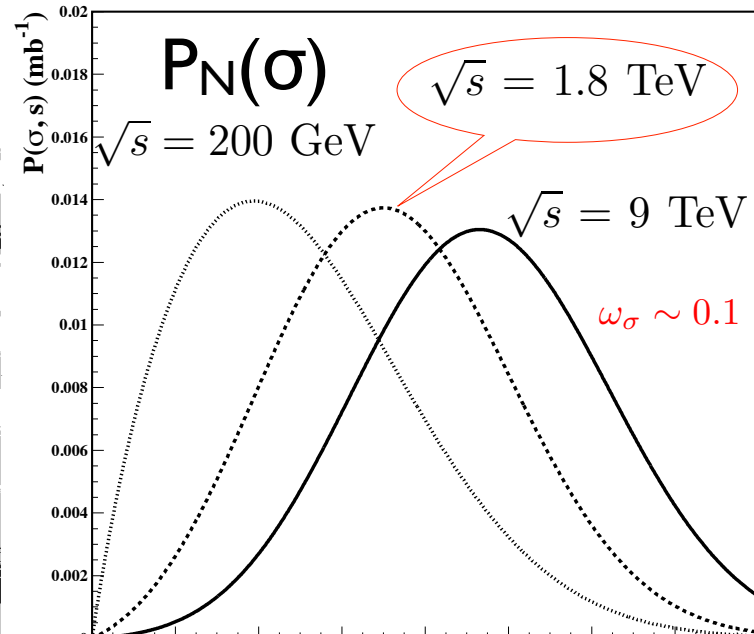
$$P_N(\sigma_{tot}) = r \frac{\sigma_{tot}}{\sigma_{tot} + \sigma_0} \exp\left\{-\frac{(\sigma_{tot}/\sigma_0 - 1)^2}{\Omega^2}\right\}$$

Test: calculation of coherent diffraction off nuclei: $\pi A \rightarrow XA, p A \rightarrow XA$ through $P_h(\sigma)$



$P_N(\sigma)$ extracted from pp,pd diffraction and $P_\pi(\sigma)$; Baym et al 93

Flat $P_N(\sigma)$ in a wide range of σ - can suggest few effective constituents at this energy scale like in quark - diquark model.



Extrapolation of Guzey & MS before the LHC data

Variance drops with increase of energy, overall shift of distribution to larger σ

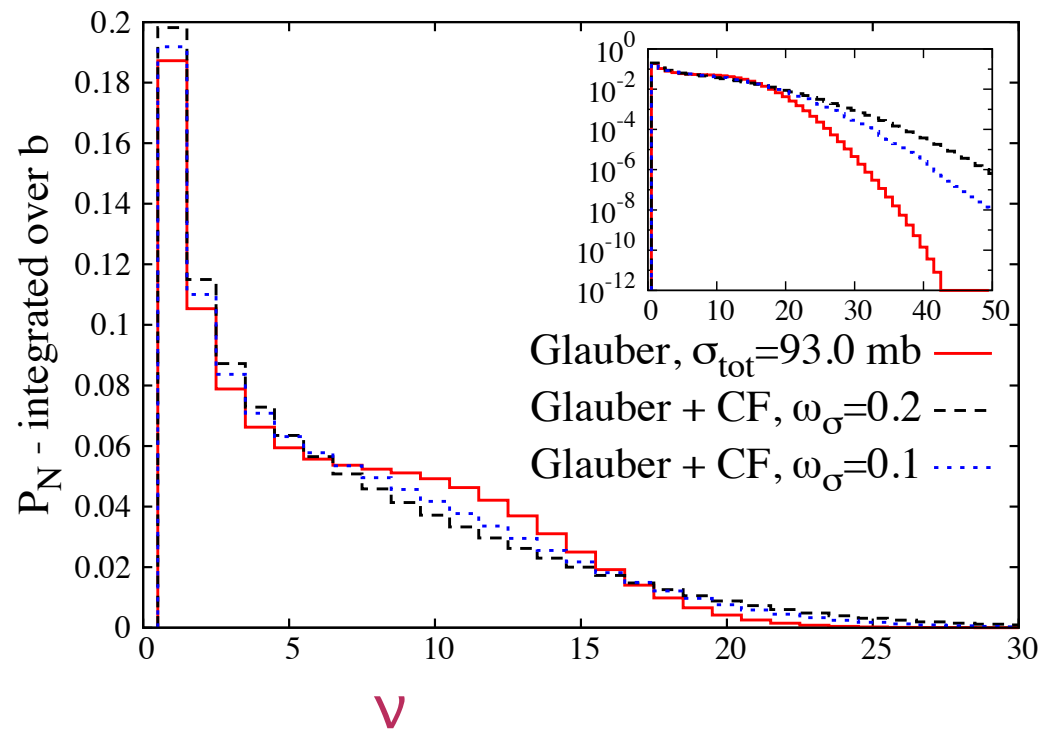
Fast drop of $P_N(\sigma)$ at small σ , with increase of energy pQCD?

Can use $P(\sigma)$ to implement Gribov- Glauber dynamics of inelastic pA interactions. Baym et al 91-93

$$\sigma_{\text{in}}^{\text{NA}} = \int d\sigma_{in} P(\sigma_{in}) \int d\vec{b} [1 - (1 - x)^A]$$

$$\sigma_n = \int d\sigma_{in} P(\sigma_{in}) \frac{A!}{(A - n)! n!} \int d\vec{b} x^n (1 - x)^{A-n} .$$

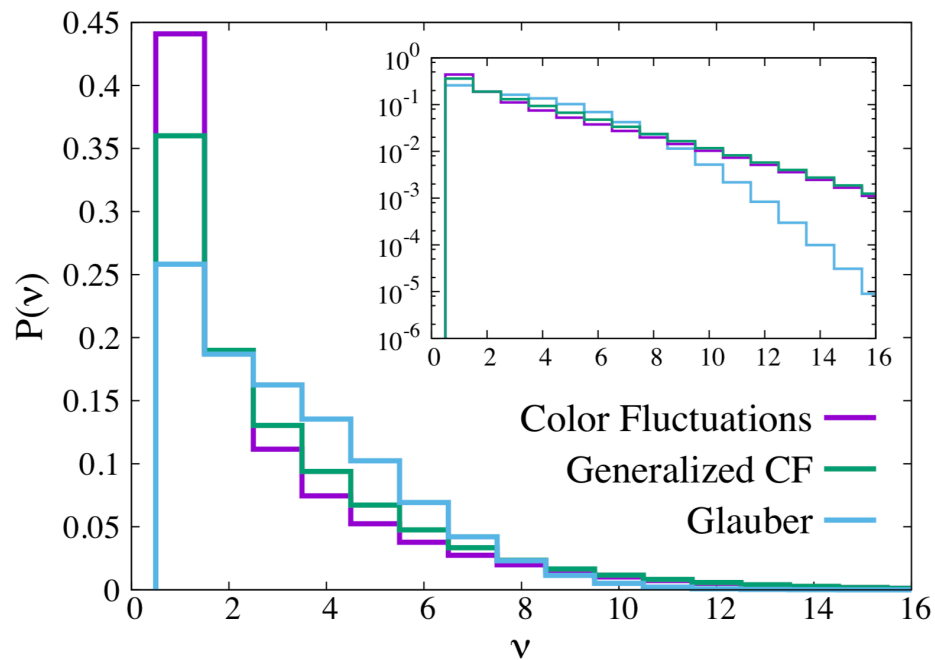
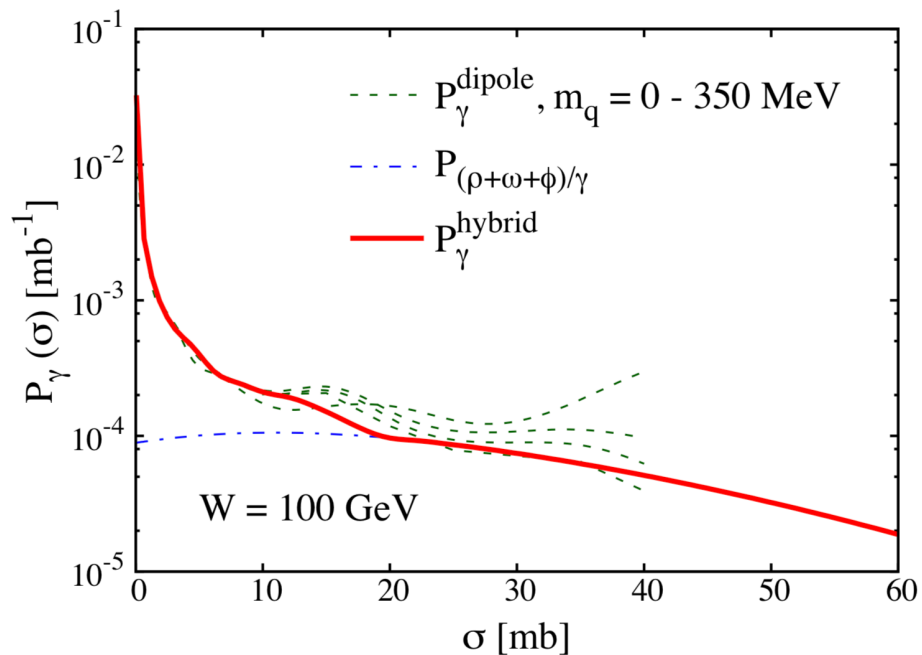
Probability of exactly n interactions is $P_n = \sigma_n / \sigma_{in}^{hA}$



Distribution over $v = N_{\text{coll}}$ is sensitive primarily to the value of variance ω_σ

ΣE_T^{Pb} distribution as a function of v : modeling by ATLAS at large negative rapidities $-3 > \eta > -5$

Similar effects in photon - nucleus collisions (a broader distribution in number of wounded nucleons) UPC & EIC



Plenty of predictions for ultraperipheral collisions at LHC

Hadron - nucleus collisions give a unique tool to go beyond single parton 3D image of the nucleon

Can study how **11D** distribution (parton density) is correlated with the overall transverse size of the nucleon.

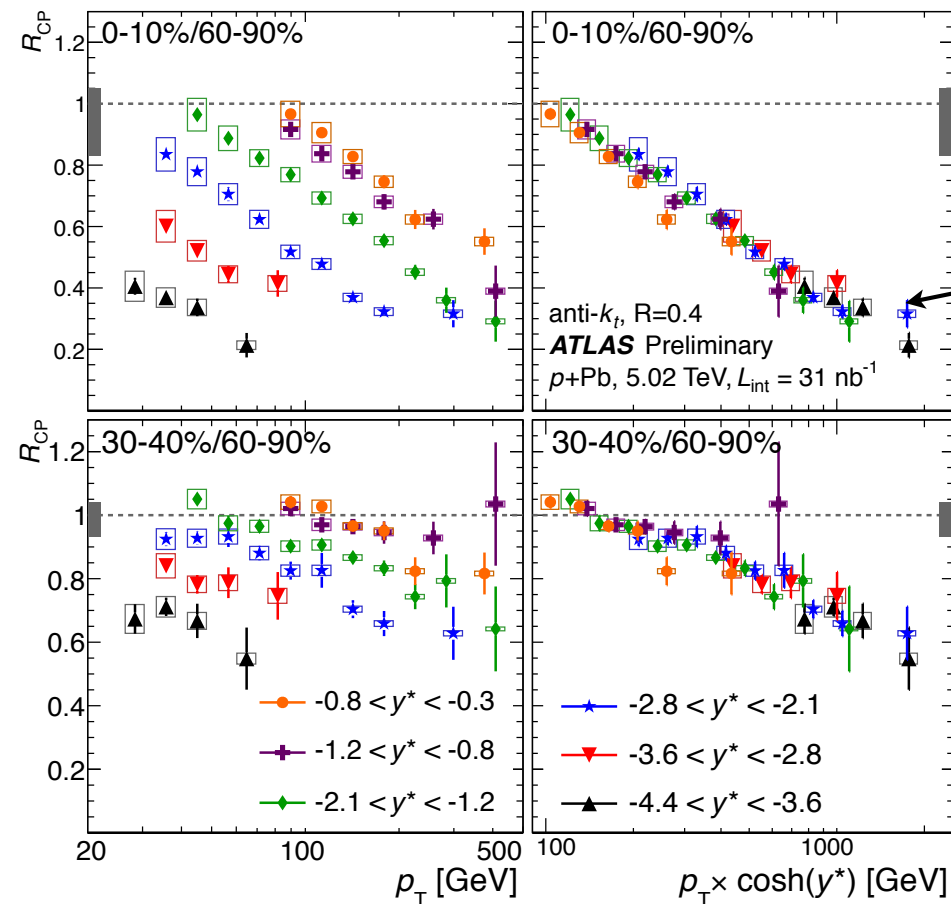
Tool: correlation between the hard and soft components of pA interaction

IDEA

Use the hard trigger (dijet) to determine **x of the parton in the proton (x_p)** and low p_t hadrons to measure overall strength of interaction **σ_{eff}** of configuration in the proton with given **x** FS83

Expectation: large x ($x \gtrsim 0.5$) correspond to smaller $\sigma \rightarrow$ drop of # of wounded nucleons, central multiplicity

ATLAS and CMS studied 5 years ago dijet production in pA at the LHC. Both observed very small nuclear effects for inclusive dijet production which rules out energy loss interpretation. However nuclear effects are strong function of N_{coll} , which was estimated using negative rapidities. Forward jet production in central collisions is strongly suppressed - suppression is mainly function of x_q , and not p_t of the jet. Consistent with expectation that configurations in protons with large x - belong to configurations which are smaller and interact with $\sigma < \sigma_{\text{tot}}$.



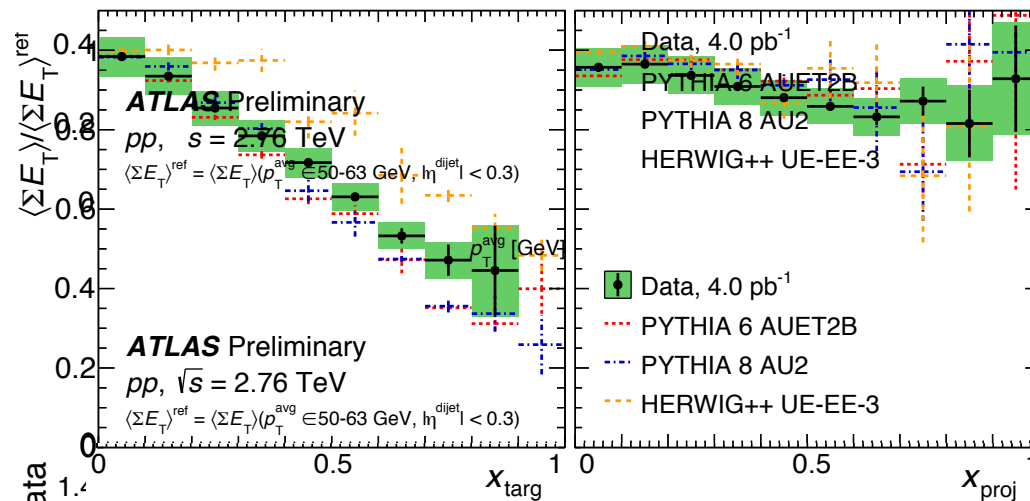
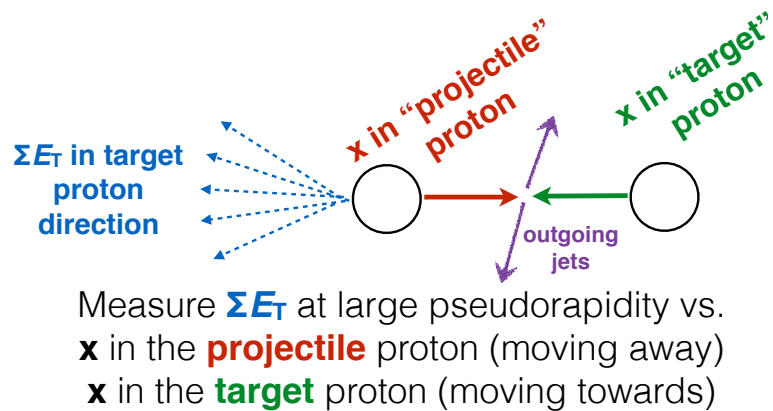
$$x_q \sim 0.5$$

R_{CP} , is a function of x of the quark. No p_T dependence for fixed x

ATLAS new data with much higher statistics

In order to compare with the data we need to use a model for the distribution in E_T^{Pb} as a function of v . We use the analysis of ATLAS. Note that E_T^{Pb} was measured at large negative rapidities which minimizes the effects of energy conservation (production of jets with large x_p) suggested as an explanation of centrality dependence

ATLAS-CONF-2015-019 analysis of pp data confirms this expectation



Dependence on x_{proj} and x_{targ}

DISTRIBUTION OVER THE NUMBER OF COLLISIONS FOR PROCESSES WITH A HARD TRIGGER

M.Alvioli, L.Frankfurt, V.Guzey and M.Strikman,
`Revealing nucleon and nucleus flickering
in pA collisions at the LHC,' arXiv:1402.2868

Consider multiplicity of hard events $Mult_{pA}(HT) = \sigma_{pA}(HT + X)/\sigma_{pA}(in)$

as a function of N_{coll}

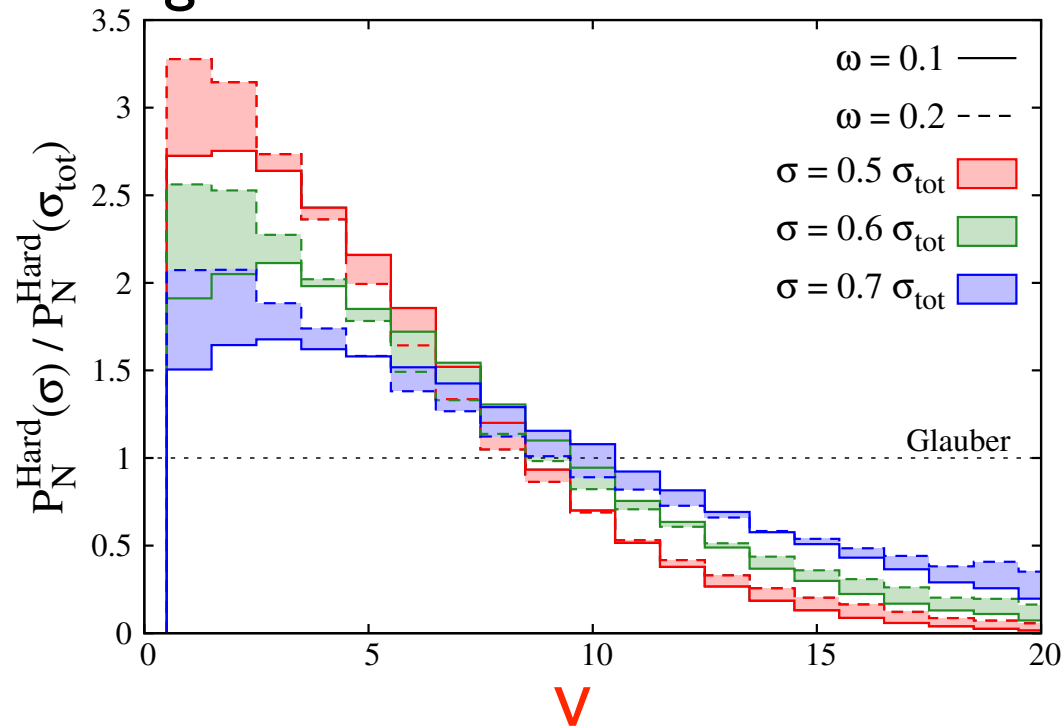
If the radius of strong interaction is small and hard interactions have the same distribution over impact parameters as soft interactions multiplicity of hard events:

$$R_{HT}(N_{coll}) \equiv \frac{Mult_{pA}(HT)}{Mult_{pN}(HT)N_{coll}} = 1$$

Accuracy?

Two effects: Two scale dynamics of soft and hard pp interaction at the LHC

Fluctuations for configurations with small σ maybe different than for average one so we considered both $\omega_{\sigma}(x \sim 0.5) = 0.1$ & 0.2

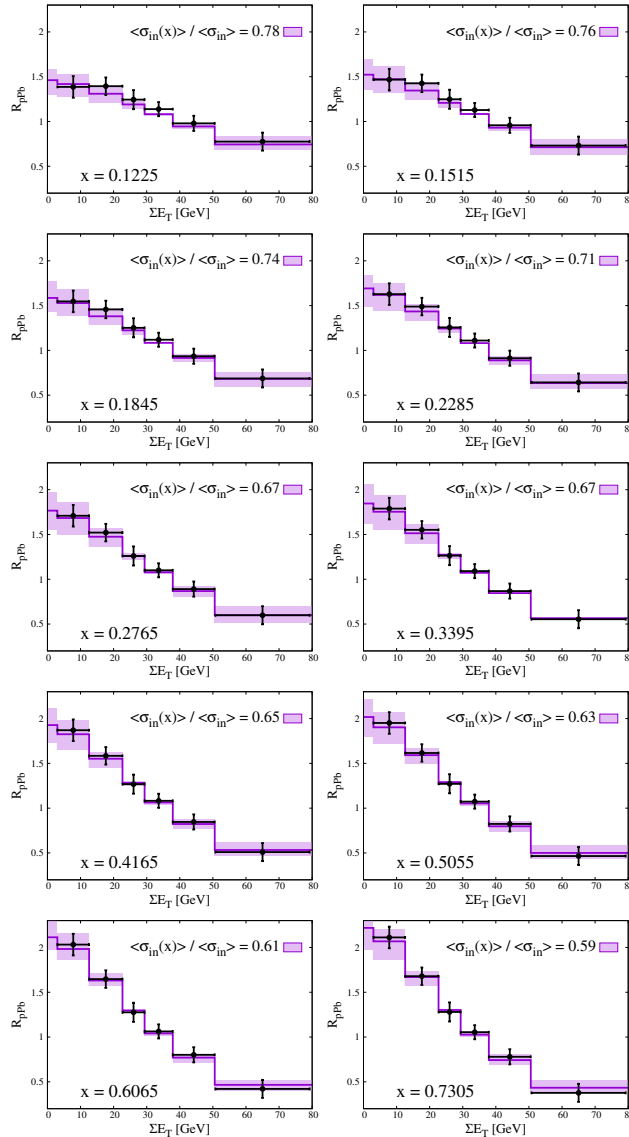


Sensitivity to ω_{σ} is small, so we use $\omega_{\sigma} = 0.1$ for following comparisons

We extended our 2015 analysis of ATLAS data and extracted $R_{CP}(x)$

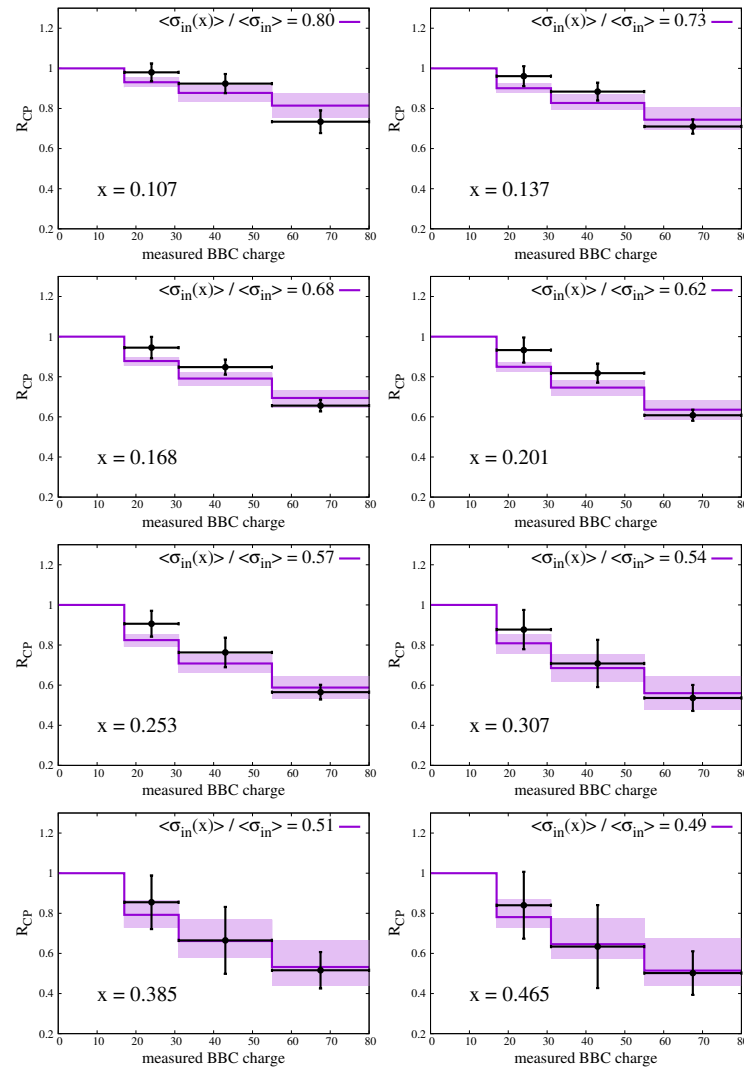
Alvioli, Frankfurt, Perepelitsa, MS Phys.Rev. D98 (2018) no.7, 071502

$$\lambda(x) = \sigma(x) / \langle \sigma \rangle$$



Deviations from Glauber model for dijets described in the color fluctuation model as due to decrease of $\langle \sigma_{\text{eff}}(x) \rangle / \sigma_{\text{in}}$

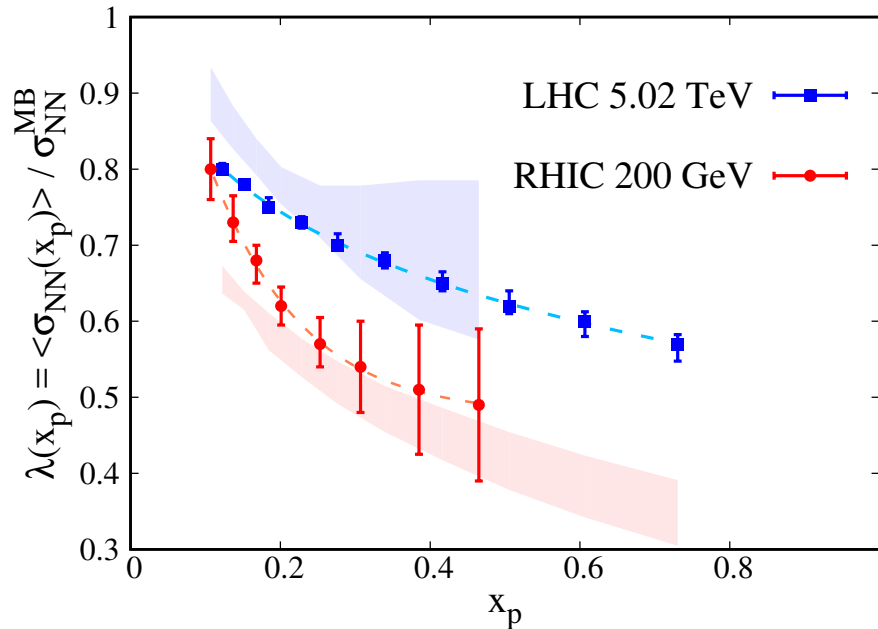
Data from pA ATLAS



DAu PHENIX data at $y=0$ and large transverse momenta of the jets, R_{CP} , $\lambda(x) = \sigma(x) / \langle \sigma \rangle$. Very different kinematics from the one studied at the LHC

Implicit eqn. for relation of $\lambda(x_p, s_1)$ and $\lambda(x_p, s_2)$

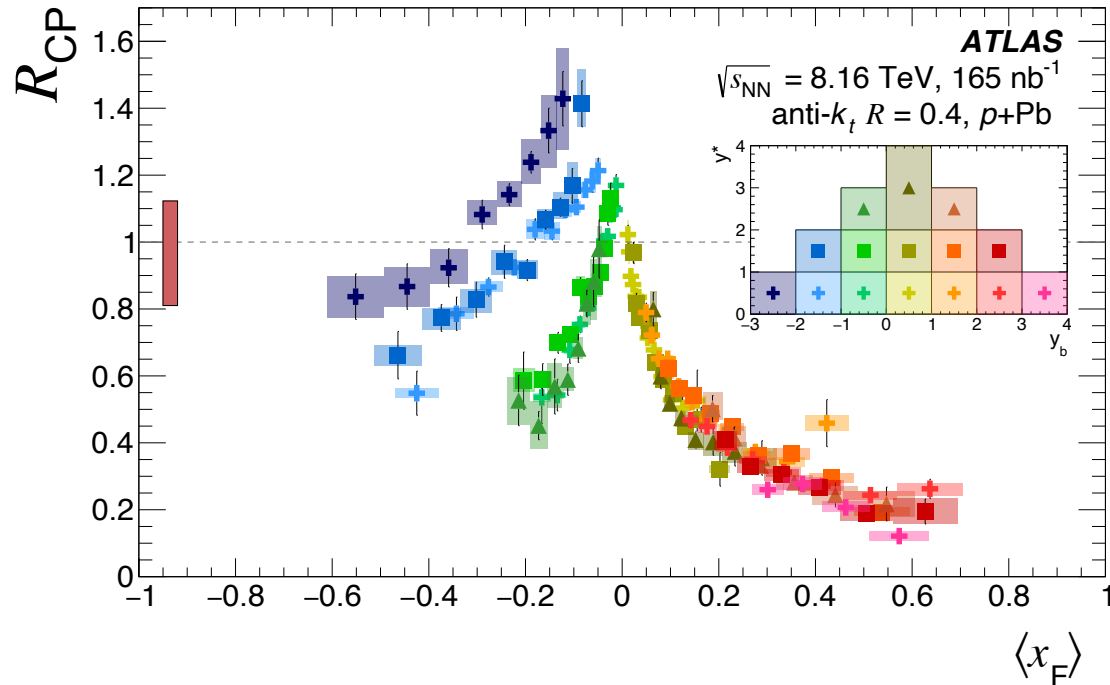
$$\int_0^{\lambda(x_p; \sqrt{s_1})} \sigma_{tot}(\sqrt{s_1}) d\sigma P_N(\sigma; \sqrt{s_1}) = \int_0^{\lambda(x_p; \sqrt{s_2})} \sigma_{tot}(\sqrt{s_2}) d\sigma P_N(\sigma; \sqrt{s_2}) \quad \text{Eq. (*)}$$



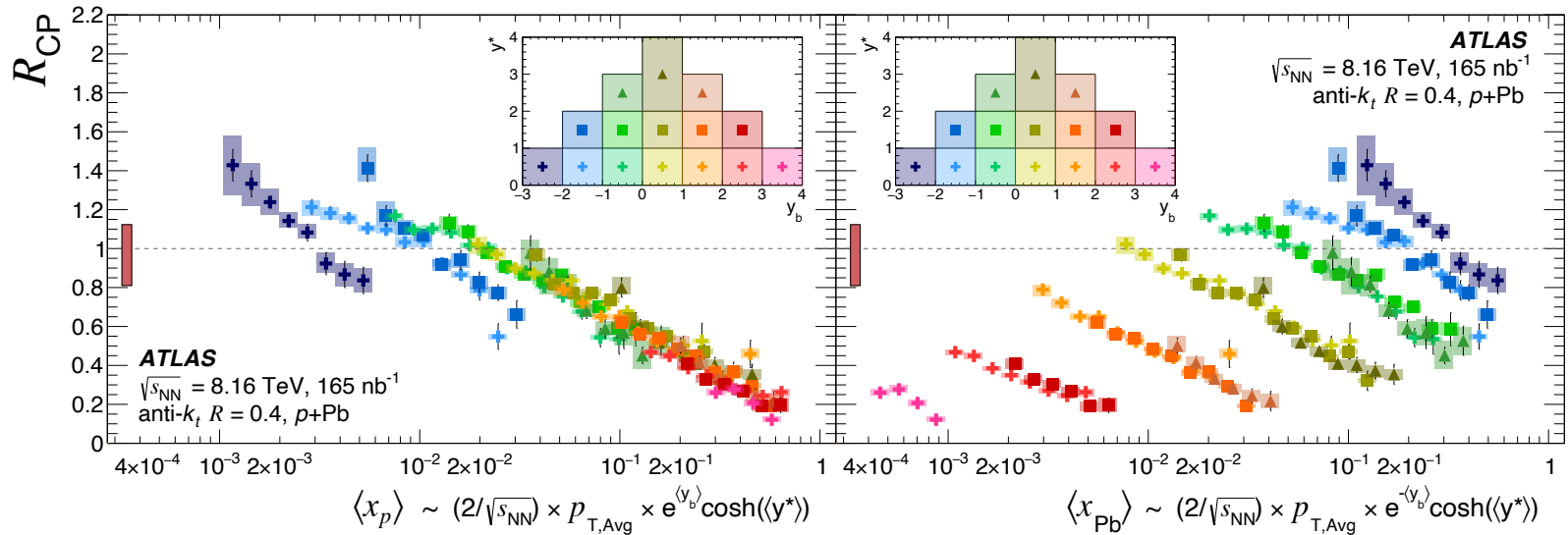
$\lambda(x_p, s)$ grows with s since cross section at higher virtualities of the projectile grows faster with s

Highly nontrivial consistency check of interpretation of the data at different energies and in different kinematics
 Eq.(*) suggests $\lambda(x_p=0.5, \text{low energy}) \sim 1/4$. Such a strong suppression results in the EMC effect of reasonable magnitude due to suppression of small size configurations in bound nucleons (Frankfurt & MS83)

$$R_{\text{CP}}(p_{\text{T,Avg}}, y_{\text{b}}, y^*) = \frac{\frac{1}{\langle T_{\text{AB}}^{0-10\%} \rangle} \frac{1}{N_{\text{evt}}^{0-10\%}} \frac{d^3 N_{\text{dijet}}^{0-10\%}}{dp_{\text{T,Avg}} dy_{\text{b}} dy^*}}{\frac{1}{\langle T_{\text{AB}}^{60-90\%} \rangle} \frac{1}{N_{\text{evt}}^{60-90\%}} \frac{d^3 N_{\text{dijet}}^{60-90\%}}{dp_{\text{T,Avg}} dy_{\text{b}} dy^*}},$$



PCP plotted as a function of approximated χ_F , here indicated with $\langle x_F \rangle$ and constructed using $\langle y_b \rangle$ and $\langle y^* \rangle$. An inset legend is included, showing the (y_b, y^*) bins, and their corresponding markers. The proton-going direction is defined by $y_b > 0$. Shaded rectangles represent the total systematic uncertainty, while the vertical error bars represent the statistical uncertainty. The solid rectangle on the left-side of the panel represents the uncertainty on the $\langle T_{\text{AB}} \rangle$.



RCP plotted as a function of approximated x_p (left panel) and y^* (right panel), constructed using $\langle y_b \rangle$. An inset legend is included, showing the (y_b, y^*) bins, and their corresponding markers. The proton-going direction is defined by $y > 0$. Shaded rectangles represent the total systematic uncertainty, while the vertical error bars represent the statistical uncertainty. The solid rectangle on the left-side of each panel represents the uncertainty on the TAB.

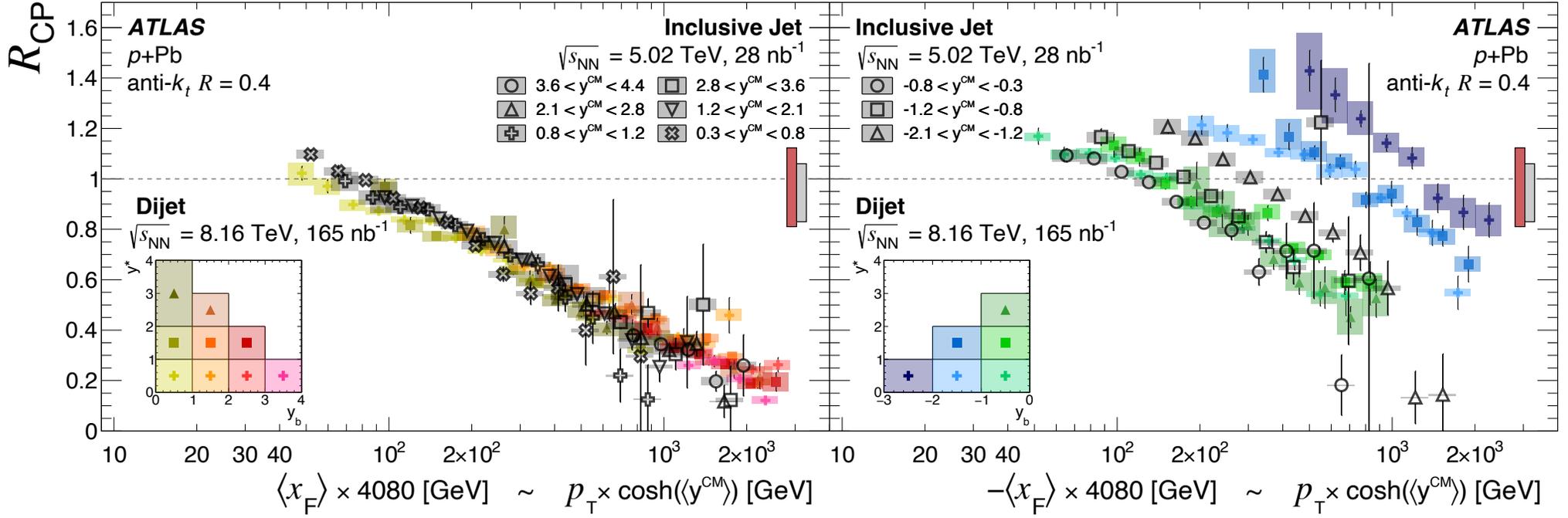


Figure 3: Dijet R_{CP} results from this Letter compared with inclusive jet R_{CP} at 5.02 TeV measured by ATLAS [9]. The dijet results are denoted by full markers and are reported as a function of $\pm \langle x_F \rangle \times 4080$ GeV, for positive (+, left panel) and negative (–, right panel) y_b (y^{CM}) results, respectively. An inset legend is included, showing the (y_b , y^*) bins, and their corresponding markers. The inclusive jet results are displayed as a function of $p_T \times \cosh(\langle y^{CM} \rangle)$ and use open markers. Shaded rectangles represent the total systematic uncertainty, while the vertical error bars represent the statistical uncertainty. The uncertainties on the T_{AB} on the dijet (inclusive jet) results are reported using the left (right) solid rectangle on the right side of each panel. The 5.02 TeV data for $-0.3 < y^{CM} < 0.3$ was omitted since it belongs to the transition region between the two panels.

Tasks for the future analyses

- * Separate gluon jets to see whether R_{CP} is different for interaction with gluon and quark — relation to the EMC effect for gluons.
- * Centrality dependence for fixed x_p and different x_A
- * BNL (RHIC) pA data for large p_{jet} and $y=0$.
- * pO (LHC)
- * fluctuations in photon - nucleus collisions - minimum bias, dijets, etc (UPC at LHC)

Forward Dipion pion data qualitatively consistent with increase of the suppression for this kinematics as the second jet is also in BDR. Stronger post selection effect - enhanced effective energy losses - *hope experiments will provide more information on centrality dependence, etc.*

Independent of details - strong evidence for breaking pQCD approximation in the kinematics sensitive to strong gluon field in nuclei. Very strong suppression of forward nucleon production in central pA collisions seems unavoidable within presented logic.

Conclusions

Generic features expected in all model in which interaction strength is comparable with black disk regime:

- ▶ Strong suppression of the large z spectra at low p_t
- ▶ Broadening of the transverse momentum distribution at large z ,

Both effects should become more and more pronounced with increase of collision energy and centrality of collision / increase of A .

Very forward pA and UPC at the LHC have a tremendous potential for probing many features of QCD including the small x dynamics. Ability to compare data at two energies (RHIC and LHC) would be highly beneficial.

Supplementary slides

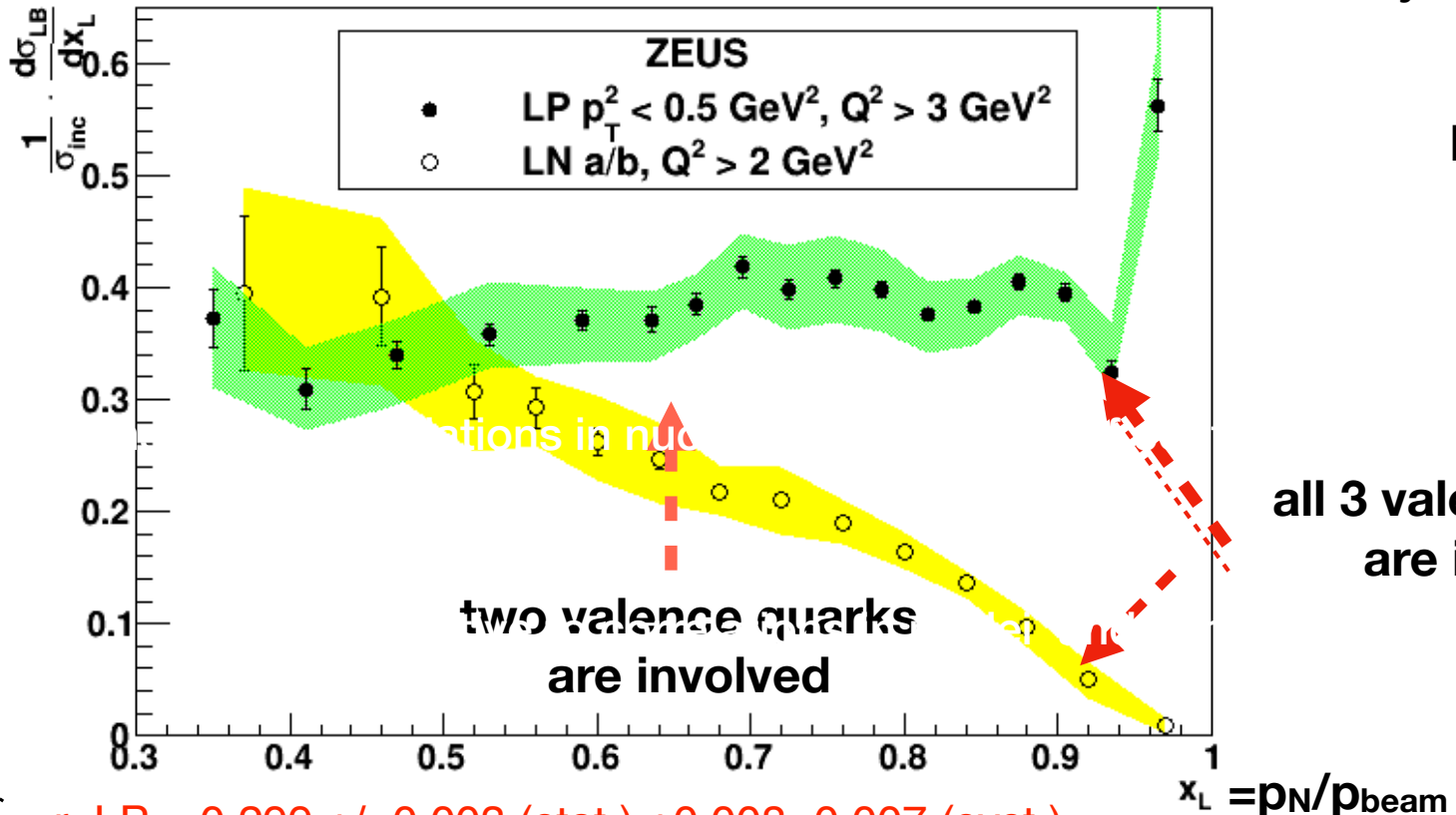
How nucleons fragment when a parton is removed by a hard probe?

sensitive to parton correlations in nucleon and to pattern of confinement

experimental studies in the scaling limit - HERA for small x.

Analysis of HERA ZEUS data

plot prepared by W. Schmidke



$r_{LP} = 0.299 \pm 0.003 \text{ (stat.)} + 0.008 - 0.007 \text{ (syst.)}$
 $r_{LN} = 0.159 \pm 0.008 \text{ (stat.)} + 0.019 - 0.006 \text{ (syst.)}$

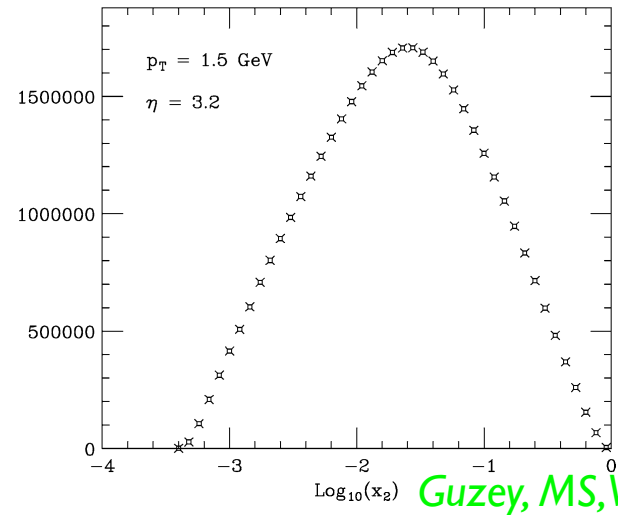
Puzzle: a lot (50%) of baryons are produced below $x_L = 0.3$ though only a small x parton was removed

Post selection and forward pion production in DAu collisions

at RHIC

For pp - pQCD works both for forward inclusive pion spectra and for correlations (STAR)

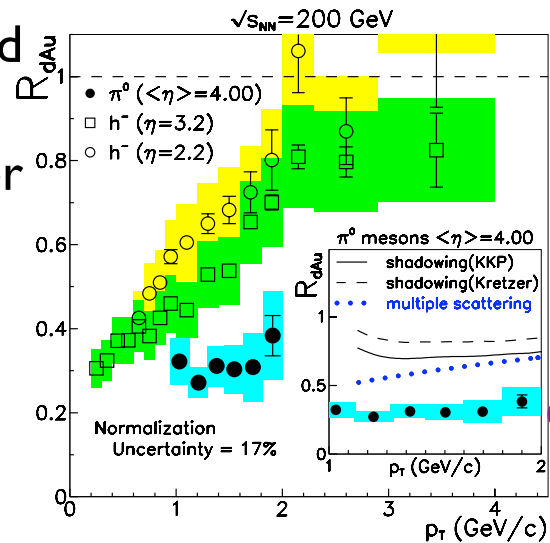
Tests that main contribution to forward pion production comes from quark scattering off gluons with $\langle x \rangle > 0.01$ which are not screened in the case of scattering off nuclei



Guzey, MS, Vogelsang 04

Fig. 1. Distribution in $\log_{10}(x_2)$ of the NLO invariant cross section $E d^3 \sigma / dp^3$ at $\sqrt{s} = 200$ GeV, $p_T = 1.5$ GeV and $\eta = 3.2$.

Suppression of the pion spectrum for fixed p_t increases increase of η_N . Dynamical suppression effect for $\eta=3.2$ is even larger than the BRHAMS ratio (by a factor of 1.5) due isospin effect.



BRAHMS and STAR are consistent when the BRAHMS data are corrected for the isospin effect

BDR up to $p_t^{(BDR)} \sim \text{few GeV}$



suppression should be larger than in eikonal rescattering CGC models -
color opacity regime

Propagation for $p_t \leq p_t^{(BDR)}$

Post-selection - effective fractional energy losses

First example: Inclusive production of leading hadrons in DIS for $Q < 2p_t^{(BDR)}$

The mechanism of fragmentation in BDR: target selects quark and antiquark in the γ^* wave function with $p_t \propto Q_{BDR}$ and known z -distribution peaked at $\sim 1/2$ fragment independently since in this case overlap between showers is small (as long as LC fractions are large).

Hence to a
first approximation

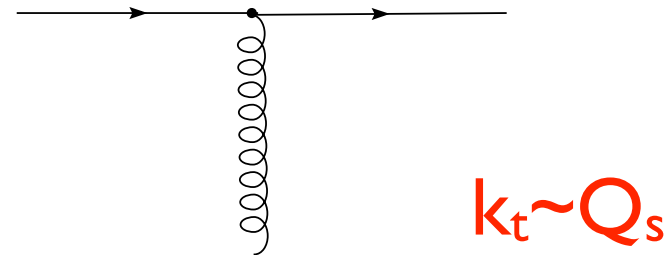
$$\bar{D}^{\gamma_T^* \rightarrow h}(z) = 2 \int_z^1 dy D_q^h(z/y) \frac{3}{4} (1 + (2y - 1)^2)$$

Gross scaling violation in BDR as compared to DGLAP. The leading particle spectrum in BDR is strongly suppressed. The inclusion of the $q\bar{q}g$ states in the virtual photon wave function (due to the QCD evolution) further amplifies the effect.

Two possible explanations both based on presence of high gluon field effects

Color Glass Condensate model

Assumes that the process is dominated both for a nucleus and nucleon target by the scattering of partons with minimal x allowed by the kinematics: $x \sim 10^{-4}$ in a $2 \rightarrow 1$ process.



Two effects - (i) density is smaller than for the incoherent sum of participant nucleons by a factor N_{part} , (ii) enhancement due to increase of k_t of the small x parton: $k_t \sim Q_s$. \rightarrow Overall dependence on N_{part} is $(N_{part})^{0.5}$, collisions with high p_t trigger are more central than the minimal bias events, no recoil jets in the kinematics expected in pQCD.

\Rightarrow **dominant yield from central impact parameters**

Energy losses in BDR regime - usually only finite energy losses discussed (BDMPS) - hence a rather small effect for partons with energies 10^4 GeV in the second nucleus rest frame. Not true in BDR - post selection - energy splits before the collision - effectively 10- 15 % energy losses.

\Rightarrow **dominant yield from peripheral impact parameters**

To use information about central rapidities in a detailed way we used the relevant information from dAu BRAHMS analysis. Results are not sensitive to details.

We confirm that pion production is strongly dominated by peripheral collisions, and that there is no significant suppression of dijet mechanism for forward-central correlation.

For central impact parameters suppression is by a factor > 5 , which requires energy losses of $> 10\%$

Since the second jet has much smaller longitudinal momentum than the jet leading to the forward pion production it propagates in a much more pQCD like regime with much smaller energy losses, and hence does not affect the rate of correlation. If the energy losses were fractional but energy independent this would not be the case.

Test of our interpretation- ratio, R , of soft pion multiplicity at $y \sim 0$ with π^0 trigger and in minimal bias events.

In CGC scenario $R \sim 1.3$

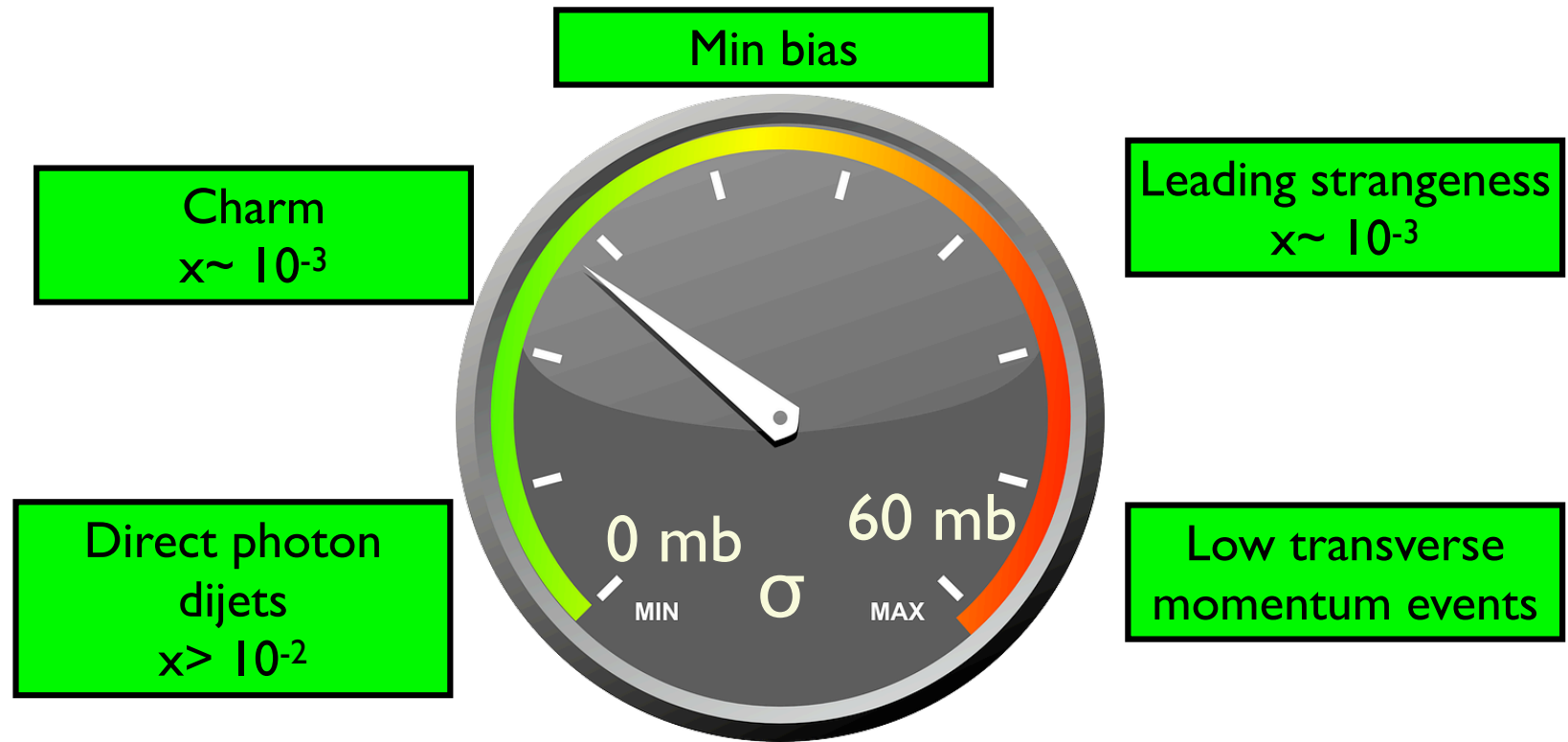
In BDR energy loss scenario we calculated $R \sim 0.5$

STAR - $R \sim 0.5$ Gregory Rakness - private communication

Further confirmation - forward-central correlation data reported by STAR and PHENIX at QM 09

Ultraperipheral collisions at LHC ($W_{\gamma N} < 500$ GeV)

Tuning strength of interaction of configurations in photon



EIC & LHeC - Q^2 dependence “*2D strengthonometer*” - - decrease of role of “fat” configurations, multinucleon interactions due to LT nuclear shadowing

Novel way to study dynamics of γ & γ^ interactions*

Summary of the challenge

☞ For pp - pQCD works both for inclusive pion spectra and for forward - central rapidity correlations

☞ Suppression of the pion spectrum for fixed p_t increases with increase of η_N . Pion production is mostly from peripheral collisions

The key question what is the mechanism of the suppression of the dominant pQCD contribution - scattering off gluons with $x_A > 0.01$ where shadowing effects are very small.

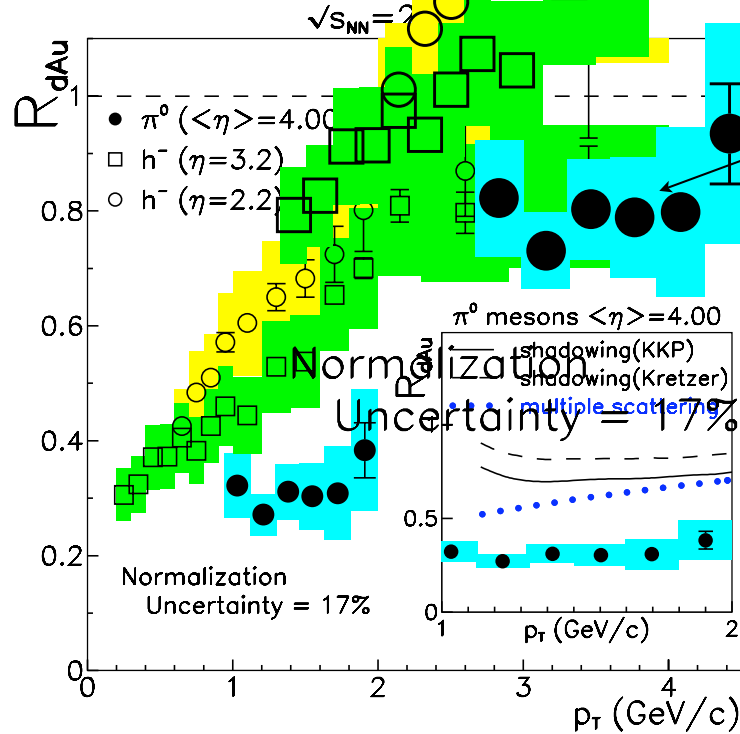
two scenarios: CGC & post-selection

**CGC: leading pions from central collisions;
post-selection - pions from peripheral collisions**

supported by soft multiplicity data

Independent of details - the observed effect is a strong evidence for breaking pQCD approximation. Natural suspicion is that this is due to effects of strong small x gluon fields in nuclei as the forward kinematics sensitive to small x effects.

Future: analysis of the A-dependence/centrality of pion production data at wide range of energies. Production of leading mesons in pp collisions with centrality trigger - like multijet production.



Significant nuclear suppression = $R_{dAu}/1.5$

BRAHMS and STAR are consistent when an isospin correction which reduces h^- ratio measured by BRAHMS by a factor ~ 1.5 (Guzey, MS, Vogelsang 04 = GSV04) is introduced

FIG. 3: Nuclear modification factor (R_{dAu}) for minimum-bias d+Au collisions versus transverse momentum (p_T). The solid circles are for π^0 mesons. The open circles and boxes are for negative hadrons (h^-) at smaller η [10]. The error bars are statistical, while the shaded boxes are point-to-point systematic errors. (Inset) R_{dAu} for π^0 mesons at $\langle\eta\rangle = 4.00$ compared to the ratio of calculations shown in Figs. 2 and 1.

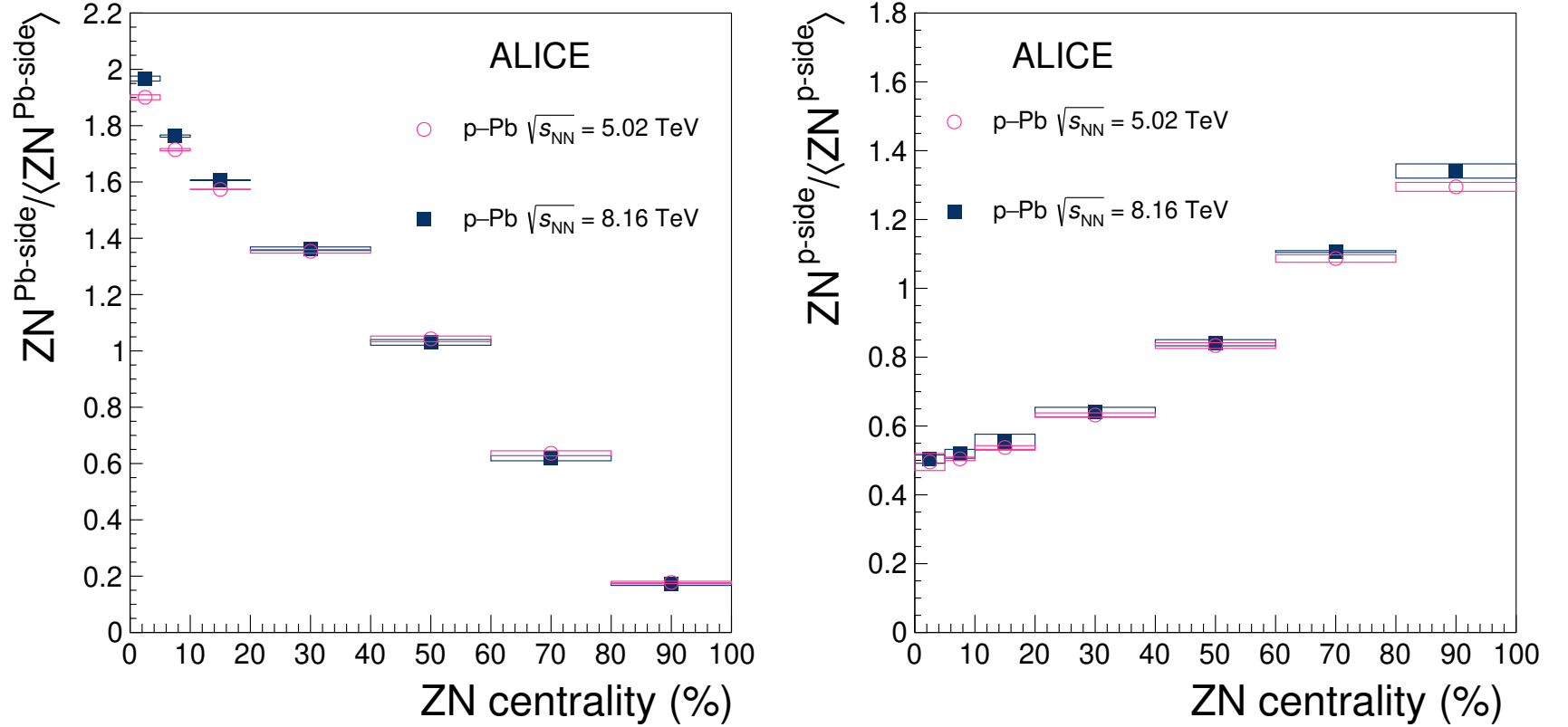


Figure 3. ZN energy normalised to the average MB value in the Pb-fragmentation (left) and in the p-fragmentation (right) regions as a function of centrality estimated from ZN [17] in p-Pb collisions at $\sqrt{s_{NN}} = 5.02$ TeV (pink circles) and 8.16 TeV (blue squares). The boxes represent the systematic uncertainty.

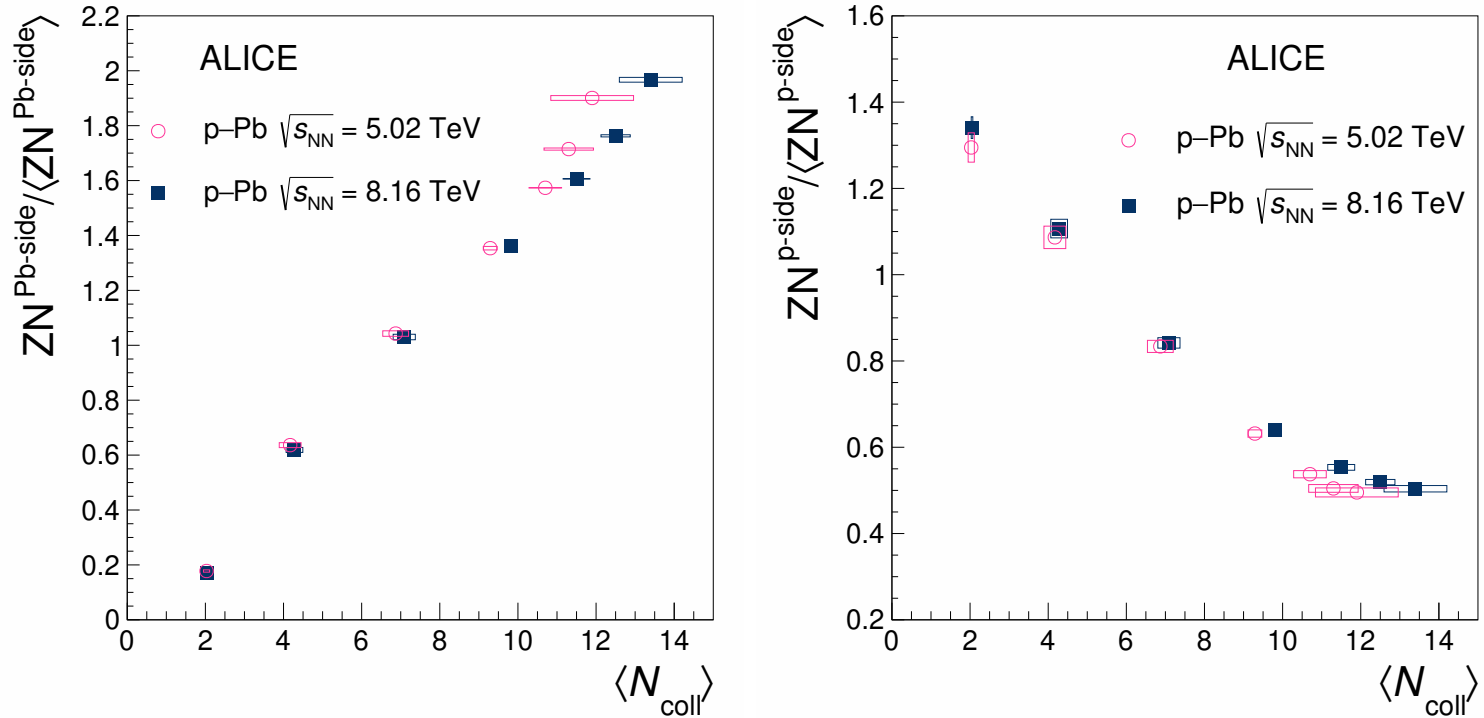


Figure 4. ZN energy normalised to the average MB value in the Pb-fragmentation (left) and in the p-fragmentation (right) regions as a function of the average N_{coll} in p-Pb collisions at $\sqrt{s_{\text{NN}}} = 5.02$ TeV (pink circles) and 8.16 TeV (blue squares). The boxes represent the systematic uncertainty.